

RESEARCH

Open Access



Enhancing electrical characteristics and electromagnetic interference shielding effectiveness in thermoplastic elastomeric polymer blends by utilizing the selective distribution of conductive black

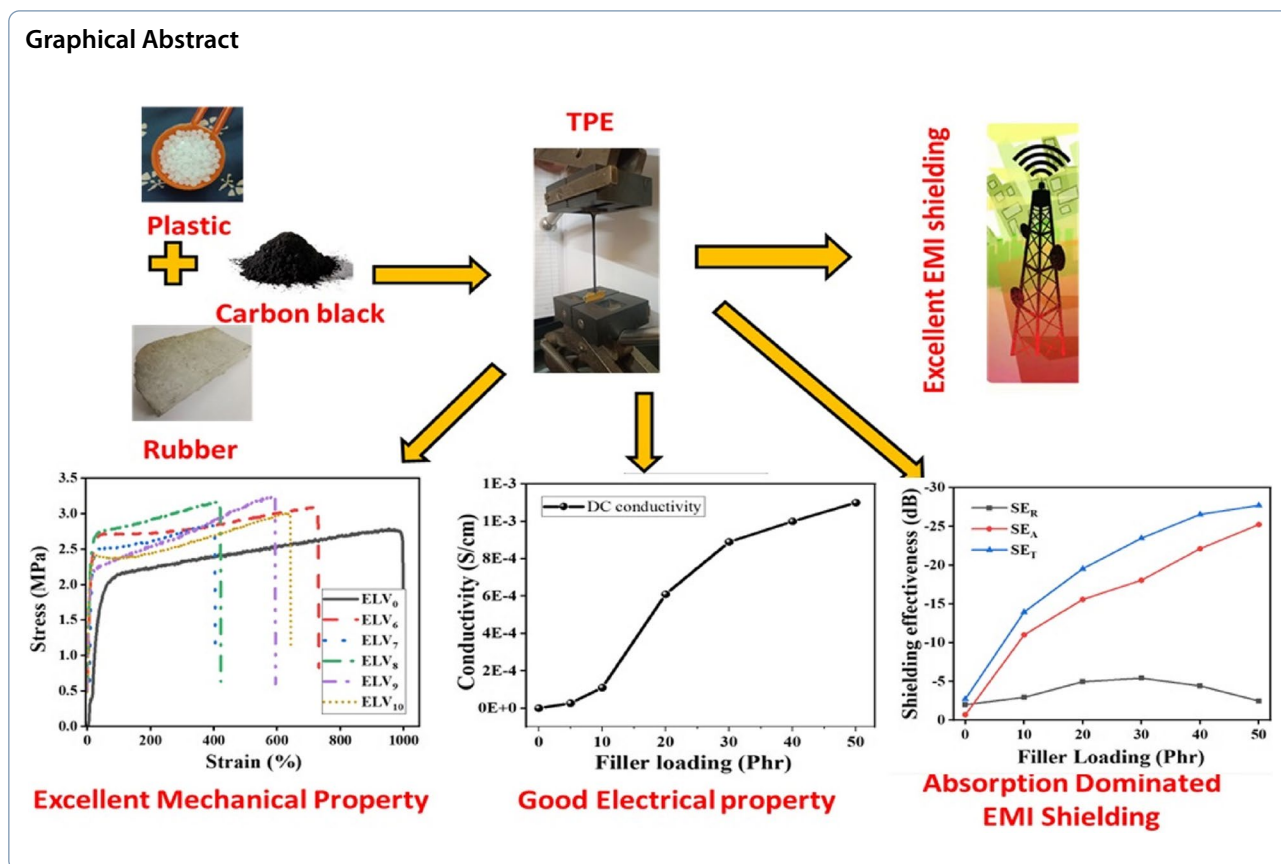
Sreeja Nath Choudhury¹, Jasomati Nayak¹, Palash Das¹, Aparajita Pal¹, Ankur Katheria¹, Pallab Banerji² and Narayan Ch. Das^{1*}

Abstract

The selective distribution of filler within polymer blends presents a compelling advantage, notably manifesting as a reduced percolation threshold when compared to an individual polymer matrix with a random filler dispersion. In this context, a thermoplastic elastomeric (TPE) blend comprising ethylene propylene diene rubber (EPDM) and linear low-density polyethylene (LLDPE), denoted as EL, has been meticulously formulated. The incorporation of varying amounts of conductive carbon black (Vulcan XC 72; VCB) into this TPE matrix has been achieved through conventional melt blending, yielding a composite material with exceptional electromagnetic interference (EMI) shielding effectiveness of -27.80 dB at 50 phr (parts per hundred rubber). This success is credited to the creation of a linked structure resulting from a dual-step percolation process. The selective distribution of carbon black (CB) throughout the TPE mixture results in a decreased critical concentration for connectivity and enhanced electromagnetic interference (EMI) shielding performance. This advancement underscores the potential of EPDM-LLDPE-VCB (ELV) composites to safeguard against electromagnetic radiation. It paves the way for their utilization in various techno-commercial applications, where a balance of mechanical strength, thermal stability, and flexibility is crucial.

Keywords Polymer blends, Conductive carbon black, Co-continuous morphology, Selective distribution, Electrical conductivity, Double percolation behavior, Electromagnetic interference shielding

*Correspondence:
Narayan Ch. Das
ncdas@rtc.iitkgp.ac.in
Full list of author information is available at the end of the article



Introduction

The widespread utilization of electronic goods has given rise to a significant and potentially harmful issue known as electromagnetic interference (EMI). EMI poses serious consequences, disrupting communication systems, posing threats to critical infrastructure, and undermining the reliability of electronic devices [1]. Moreover, aside from its impact on electronic devices, EMI can occasionally cause catastrophic catastrophes in terms of money, energy, and human life [2, 3]. Addressing EMI is essential to safeguard the functionality and safety of modern society. Historically, metals have been favored for electromagnetic interference (EMI) shielding. However, their use in aircraft and modern smart electronics is limited due to their rigidity, ease of machining, proneness to corrosion, and significant weight [4], in contrast to polymers [5]. Alternatively, certain ceramic materials, like SiC and Si₃N₄, have shown potential as effective substitutes. These materials have an adjustable microstructure at multiple scales and can be made using the right techniques [6]. The negative aspects of employing ceramics in EMI shielding applications are brittleness, restricted flexibility, weight, cost, relatively low electrical conductivity, difficulty in machining, and restrictions in shielding

efficiency at specific frequencies [7], which may make ceramics less suitable. When compared to other alternatives, polymeric materials are advantageous due to their flexibility, electrical insulation, cost-effectiveness, ease of machining, resistance to environmental factors, and suitability for a wide frequency range [8, 9].

Thermoplastic elastomers (TPEs) are a unique category of polymers having combined properties of thermoplastics and elastomers. They are composed of two constituents: a soft and flexible component and a hard and rigid component, which can be either amorphous or semi-crystalline. Hence, TPEs possess similar properties to rubbery substances and can undergo melting treatment similar to conventional thermoplastics [10, 11]. It should be noted that rubber-plastic blends only qualify as TPEs when they acquire key characteristics of rubbers, such as high elongation (>100%) and low tension set (50%) qualities [12, 13].

Achieving high electrical conductivity is crucial for the development of cost-effective electromagnetic interference (EMI) shielding materials. This is accomplished by integrating conducting fillers into polymer composites [14]. Conductive carbon-based fillers are commonly employed in the production of conducting polymer

composites to secure the required electrical properties and efficient EMI shielding [15]. In the past few years, a range of carbon-based nanofillers has been extensively adopted as conductive enhancers in polymer composites tailored for shielding effectiveness. These include conductive carbon black (CB), carbon nanofibers (CNF), graphene oxide (GO) [16, 17], multi-walled carbon nanotubes (MWCNT) [18–20], and graphene nanoplatelets (GNP) [21], along with combinations of two or more types of fillers, referred to as hybrid nanofillers [22, 23]. For a conducting polymer composite to be deemed commercially viable for electromagnetic shielding, it must exhibit an EMI shielding effectiveness (SE) of at least -15 dB. It's particularly important to measure EMI shielding in the X-band frequency range (8.2–12.4 GHz), as this is where most critical economic and military electronic devices operate [24]. A key factor in designing conducting polymer composites (CPC) is determining the electrical percolation threshold, which is the filler loading level at which the material transitions from insulating to conducting. Beyond this threshold, conductive pathways form throughout the polymer matrix [25, 26]. An effective strategy for significantly reducing the electrical percolation threshold is to use an immiscible binary polymer blend with a co-continuous morphology, facilitating the double percolation phenomenon. Double percolation, which involves the selective distribution of filler particles in one phase of a co-continuous blend, enhances electrical conductivity and shielding effectiveness [27]. Employing a thermoplastic elastomer (TPE) with co-continuous morphology also offers additional advantages in terms of material processing and reproducibility.

The polymer blend composites by combining carbon black (CB) or chemically treated surface modified nanofillers (*f*-CNT, *f*-CNF) with a binary blend of polystyrene (PS) and ethylene methyl acrylate copolymer (EMA) were prepared [28]. The PS/EMA blend exhibits a co-continuous morphology, with the preferential filler particles distribution in the EMA phase. The composite film exhibits shielding efficiency (SE) of -31 dB when loaded with 15 wt% of *f*-CNT. Ma et al. [26] researched a stretchable conductor made of isotactic polypropylene (PP) and ethylene propylene diene rubber (EPDM). They have fabricated both thermoplastic elastomers (TPE) and thermoplastic vulcanizates (TPV) by incorporating multi-walled carbon nanotubes (MWCNT) as conductive fillers. In the case of the TPE sample, a co-continuous phase was observed whereas, for TPV samples, due to the vulcanization of EPDM, the rubber phase shows a dispersion in the PP matrix with a few hundred nanometers MWCNT was located in EPDM for the TPE sample which is following the prediction of thermodynamic steady state. TPE samples show an EMI SE of -25.1 dB,

whereas TPV samples show 29.8 dB, 18.7% higher than their TPE counterparts. Chowdhury et al. [29] worked on an EMA/ carboxylated nitrile rubber (XNBR) based TPE blend. They made the conductive composite using conductive carbon black (Vulcan XC 72). The composite shows a percolation threshold at 12.5 wt% of conductive filler, and the shielding effectiveness of the conductive filler is -33.5 dB of 2 mm thick sheet for 45 phr (parts per hundred rubber) filler loading. A blend of EPDM and (Ultralow density polyethylene) ULDPE was used by Karekar et al. in their work. They used a fixed 60:40 EPDM/ULDPE ratio while working. EPDM and ULDPE exhibit continuous morphology along with thermoplastic elastomeric properties of the blend [30]. Das et al. worked on an MXene-based super stretchable elastomeric composite, reaching SE up to -27.4 dB in the X-band range [31, 32]. Katheria et al. worked on EMA/thermoplastic polyolefins (TPO) based flexible thermoplastic elastomeric blend where they used MWCNT as a conducting filler and reached a SE of about -35 dB by adding 15 wt% filler in the frequency range 14.5–20.0 GHz [33, 34].

To create TPEs, semi-crystalline polymers are typically melted and mixed with the necessary quantity of elastomers using an internal mixer or extruder. When TPEs are melted together, the high shear stress and temperature can produce rubber domains that are well distributed and of good size homogeneity across the continuous plastic matrix. The melt mixing method is typically used to create TPEs since it is efficient, doesn't require any solvents, and is appropriate for industrial manufacturing [35–37].

The primary aim of this study is to develop a lightweight composite with high conductivity and a percolated structure for effective electromagnetic interference (EMI) shielding and thermal regulation, leveraging the benefits of thermoplastic elastomers (TPEs). EPDM rubber, known for its excellent thermal stability and resistance to weathering, is selected for its widespread use in sealing applications, highlighting its suitability for such roles. Conversely, LLDPE, a thermoplastic polymer, is recognized for its remarkable flexibility, ease of processing, and broad accessibility. However, the synergistic use of EPDM rubber and LLDPE in EMI shielding applications has not been extensively explored. Thus, we utilized melt mixing to create binary polymer blends and their nanocomposites to minimize processing expenses and enhance the interaction between polymer and filler. We chose an EPDM/LLDPE (60:40 w/w) blend as a prototype blend system, which exhibits a co-continuous phase morphology and TPE-like properties. The critical concentration for forming conductive pathways is identified at 15 wt% Vulcan-XC 72 carbon black. The resulting hybrid composite films are suited for use as electromagnetic wave absorbers in wearable technology.

Experimental

Materials

The linear low-density polyethylene (LLDPE) available on the market, branded as Halene-L 7300 T, features a density of 0.934 g/cc, a melting point of 130 °C, and a melt flow index (MFI) of 120.0 g/10 min according to ASTM D1238 standards, and was sourced from Haldia Petrochemicals, India. Ethylene propylene diene rubber (EPDM), which contains 68 wt% ethylene and 5 wt% ethylidene norbornene (ENB), and has a Mooney viscosity of ML(1+4) at 100 °C of 64 Mooney units, was acquired from SUMITOMO Chemicals, Asia. The conductive carbon black known as Vulcan XC 72 (VCB), with a BET surface area of 254 m²/g, was supplied by CABOT, India.

Nanocomposite preparation

EPDM-LLDPE composites filled with different dose of Vulcan Carbon Black (VCB), were prepared using a Brabender plasticoder internal mixer (PLE-330), with the rotor speed set consistently at 70 rpm and the temperature held at 160 °C. Initially, LLDPE was pre-softened in the mixer for 2 min. Subsequently, EPDM was added and blended with LLDPE for an additional 5 min to ensure uniform mixing of them within the mixing chamber (referenced in Table 1). For the preparation of the EPDM-LLDPE-VCB composite, a calculated amount of VCB was then introduced and stirred in for another 5 min to form an even composite blend. The details blend composition is presented in Table 2. The blends were formed into sheets by the compression molding press (Moore press, UK), keeping a constant pressure of 5 MPa and a temperature of 160 °C.

Each blend without filler is labeled as “EL”, with “E” denoting EPDM and “L” signifying LLDPE, while the composites containing filler are marked as “ELV”, with “V” indicating Vulcan XC 72. The EL6040 designation refers to a pure blend composed of 60% EPDM and 40% LLDPE. The specific names for all samples are listed in Tables 1 and 2.

Table 1 Composition of EPDM/LLDPE (EL) blend with their corresponding ratio

| Sample Code | EPDM (wt%) | LLDPE (wt%) |
|-------------|------------|-------------|
| EL2080 | 20 | 80 |
| EL3070 | 30 | 70 |
| EL4060 | 40 | 60 |
| EL5050 | 50 | 50 |
| EL6040 | 60 | 40 |
| EL7030 | 70 | 30 |
| EL8020 | 80 | 20 |

Table 2 Composition of EL and VCB composites with their corresponding ratio

| Sample Code | EPDM (wt%) | LLDPE (wt%) | VCB (phr) |
|-------------|------------|-------------|-----------|
| ELV0 | 60 | 40 | 0 |
| ELV 6 | 60 | 40 | 10 |
| ELV 7 | 60 | 40 | 20 |
| ELV 8 | 60 | 40 | 30 |
| ELV 9 | 60 | 40 | 40 |
| ELV10 | 60 | 40 | 50 |

Characterization methods

The mechanical properties of both the unfilled and VCB-infused EPDM-LLDPE composites were evaluated with a universal tensile testing machine (Hounsfield H10 KS), operating at a steady crosshead speed of 500 mm per minute, in accordance with ASTM D412 and D624 guidelines. The reported results represent the mean values from three dumbbell-shaped test specimens. The structure and distribution of the filler within the polymer blends were examined using a field emission scanning electron microscope (FESEM, Merlin, Carl ZEISS Pvt Ltd.) at an acceleration voltage of 5 kV. Morphological analysis via FESEM involved cryo-fracturing the samples and scanning their fractured surfaces. The influence of filler content on the electrical conductivity of the EPDM-LLDPE blend (EL) was gauged by recording changes in direct current (DC) resistivity at a stable normal temperature of 25 ± 2 °C, comparing unfilled and filler-augmented composites. Resistivity measurements for samples conducted using digital multimeters (Agilent 4339B and Agilent 34401A 6½). An AC impedance analyzer (Win data Novotherm Alpha) was employed for assessing AC conductivity in the composites, which, along with DC conductivity, was measured on circular samples (13 mm diameter and 2 mm thickness). The electromagnetic interference shielding effectiveness (EMI SE) of all filled composites, each 2 mm thick, was determined using a Vector Network Analyzer (N9926A, Agilent Technologies, USA) across the 8.2–12.4 GHz frequency range (X-band), using a suitable waveguide. Measurements of EMI SE, along with return, absorption, and reflection loss, were taken. These tests (conductivity and EMI shielding) were replicated on three samples from each category to ensure consistency. Thermal properties of the samples were analyzed using a differential scanning calorimeter (DSC, Q2000 V24.10, TA Instruments, USA) and a thermogravimetric analyzer (TGA, Q5000, TA Instruments, USA) under nitrogen. The DSC test involved heating and cooling at a rate of 10 °C per minute from –120 °C to 200 °C, while TGA was conducted from

room temperature up to 600 °C at a steady heating rate of 10 °C per minute.

Results and discussion

Analysis of mechanical property

The mechanical properties and tensile set of EPDM/LLDPE blend (EL8020, EL7030, EL6040, EL5050, EL4060, EL3070, EL2080) are listed in the Table 3.

Low-density polyethylene (LLDPE) is a polymeric material distinguished by its linear configuration and limited lateral branching. The close alignment of its molecular chains, facilitated by this linear structure, contributes to increased intermolecular forces, including Van der Waals forces, and a greater level of crystallinity. An important characteristic of high crystallinity is its role in enhancing tensile strength, as the chains that are densely packed provide more robust resistance to external forces. In contrast to alternative polyethylene variants, long chain length polyethylene (LLDPE) features a reduced number of branches on its molecular chains, which enhances intermolecular interactions and contributes to its superior tensile strength. Furthermore, it should be noted that LLDPE is classified as a semicrystalline substance, as opposed to EPDM (Ethylene Propylene Diene Monomer), which has an amorphous structure. To increase the modulus and tensile strength of the EPDM/LLDPE (EL) composite, the existence of crystalline regions within LLDPE is a prerequisite. This observation confirms that augmenting the LLDPE concentration in the EPDM/LLDPE blend results in a concomitant augmentation of the blends' rigidity. Consequently, the value of ultimate tensile strength increases proportionally (Table 3). A progressive reduction in strain at failure is observed as the proportion of the blend's plastic phase (LLDPE) increases. This observation provides confirmation that the stiffness of the composites is enhanced by LLDPE, resulting in a corresponding decrease in the strain at break value. Literature and previously published research indicates that rubber/plastic composites with

a minimum strain at break of 100 percent and tensile set below 50 percent are classified as TPE. Therefore, it is observed that the strain at break for EL8020, EL7030, EL6040, EL5050, and EL4060 exceeds 100% (Table 3, Fig. 1a, b). The blend components' minimal polarity difference results in an admirable strain at break across a variety of compositions.

Additionally, the tensile set is a critical mechanical property of TPE. Rubber typically exhibits lower set values due to its viscoelastic characteristics. The plastic component in a blend initially strengthens the blend and helps to revert to the initial position when stress is removed. When the plastic wt% is too high, it is hard to elongate the material to 100% strain because before 100% strain archives, either failure occurs or necking has started. Hence, the set properties cannot be measured for high plastic content blend. EL8020 and EL7030 blends show a very high strain at the break due to the EPDM-rich phase in the blend. It has comparatively low ultimate tensile strength and a higher tensile set (Table 3). Due to the rubber-rich component in the blend, it shows a higher tensile set. Thus, these two blends are not taken for further Investigation. EL3070 and EL2080 blends offer a deficient strain at the break due to the LLDPE's rich phase in the blend. Thus, these two blends do not meet the criteria for being a TPE, so these two are emitted for further Investigation. EL6040, EL5050, and EL4060 show a commendable strain at the break, but it is interesting to note that EL6040 shows a tensile set less than 50%, i.e., 42.37%, and strain at break is much greater than 100%. Therefore, the EL6040 blend is taken for detailed Investigation by adding different ratios of VCB as a conducting filler to make a composite for EMI shielding application.

Improving the mechanical properties is a key reason for blending elastomeric and thermoplastic materials. Different rubbers combining different grades of plastic have been proven beneficial for tensile, aging, or abrasion properties. In this study, we consider the effect of Vulcan XC 72, conducting black filler loading on the mechanical properties of the thermoplastic elastomer (Fig. 1c, d). The analysis of the material characteristics observed through standardized uniaxial tensile testing, comparing tensile strength and elongation at break at varying conductive carbon loading in the thermoplastic elastomer, reveals essential insights into the material's behavior. At 0 phr, specifically without adding carbon black, the material exhibits a tensile strength of 4.7 MPa and an elongation at break 771%. This data establishes a baseline for the material's performance without any reinforcement. A noteworthy transformation is observed upon the introduction of carbon black as a reinforcing agent. There is a marked decrease in elongation at break, accompanied by a significant increase in tensile strength (Table 4).

Table 3 Mechanical properties of EPDM/LLDPE (EL) blend

| Sample code | Tensile Strength (MPa) | Strain at break (%) | Stress at 100% strain (MPa) | Tensile Set (%) |
|-------------|------------------------|---------------------|-----------------------------|-----------------|
| EL8020 | 3.23 | 1132 | 1.51 | 66.53 |
| EL7030 | 3.73 | 876 | 1.72 | 55.78 |
| EL6040 | 5.30 | 771 | 3.25 | 42.76 |
| EL5050 | 6.35 | 656 | 4.86 | 55.25 |
| EL4060 | 6.37 | 357 | 5.31 | 60.59 |
| EL3070 | 7.67 | 195 | 6.50 | - |
| EL2080 | 9.71 | 110 | 9.15 | - |

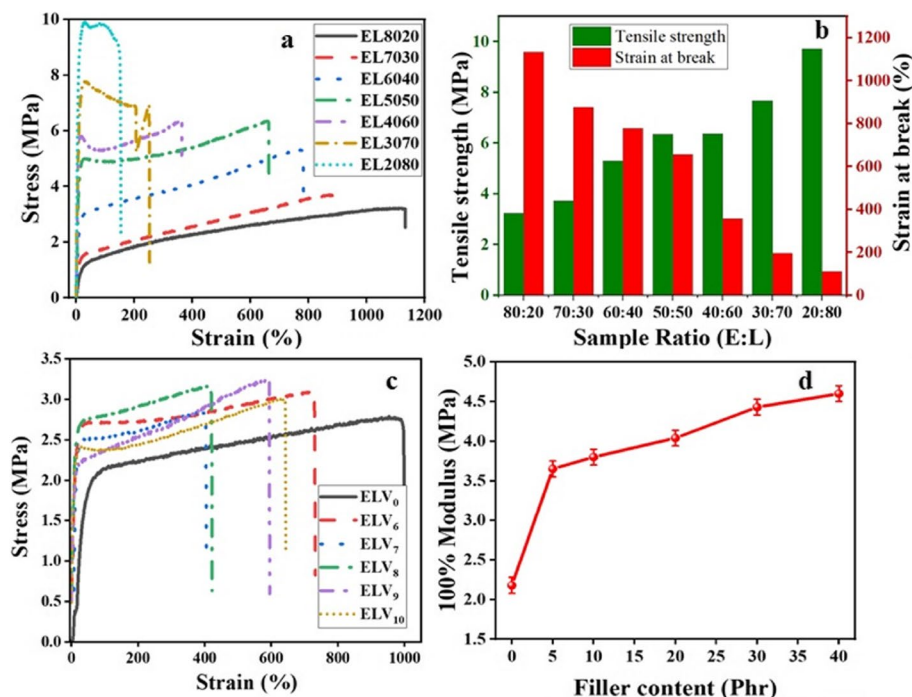


Fig. 1 a Stress-strain plot of unfilled EL blend; b Comparative study of Ultimate tensile strength and elongation at break of unfilled EL blend; c Stress-strain plot of filled ELV composites with variable filler; d 100% modulus vs filler loading

Table 4 Mechanical properties of EPDM/LLDPE/VCB composites

| Sample designation | Tensile Strength (MPa) | Tensile Strength increment (%) | Strain at break (%) | Modulus@ 100% (MPa) |
|--------------------|------------------------|--------------------------------|---------------------|---------------------|
| ELV 0 | 4.7 ± 0.05 | - | 771 ± 10 | 2.6 |
| ELV 6 | 4.9 ± 0.04 | 4.25 | 200 ± 12 | 4.6 |
| ELV 7 | 5.2 ± 0.06 | 10.63 | 235 ± 8 | 5.2 |
| ELV 8 | 5.6 ± 0.05 | 19.14 | 132 ± 10 | 5.7 |
| ELV 9 | 6.0 ± 0.03 | 27.65 | 115 ± 11 | 6.0 |
| ELV 10 | 6.2 ± 0.05 | 31.91 | 115 ± 6 | 6.3 |

This phenomenon highlights the enhanced strength and dimensional stability achieved by incorporating carbon black into the thermoplastic elastomer matrix. The data clearly illustrates a direct correlation between the quantity of carbon black added and the resultant mechanical properties. As carbon black loading increases, there is a consistent rise in ultimate tensile strength (Table 4). However, this increment in strength is counterbalanced by a gradual decrease in elongation at break. This behavior can be attributed to the optimal filler reinforcement within the blend component. This trend can be attributed to the presence of carbon black, which restricts the mobility of the EPDM rubber in the blend, causing the samples to fail at lower elongations. Carbon black

imparts stiffness to the rubber, making it less deformable under stress. It is important to emphasize that the material’s mechanical properties are intricately linked to how the filler component, i.e., carbon black, is incorporated and distributed within the thermoplastic elastomer matrix. The improvements in tensile strength and dimensional stability underscore the significance of achieving an ideal dispersion and alignment of the filler material within the composite.

Differential Scanning Calorimetry (DSC) analysis

Differential Scanning Calorimetry (DSC) analysis is pivotal for identifying two main transition temperature of polymeric material i.e. the melting temperature (Tm)

and glass transition temperature (T_g), providing insight into their unique interactions and relaxation dynamics within polymer composites. The study of how filler content influences T_g and T_m is facilitated by examining the DSC traces during the second heating of both unfilled EL blends and ELV composites with varying Vulcan Carbon Black (VCB) content, as illustrated in Fig. 2. The DSC results reveal that the EL blend exhibits a singular T_g , indicative of a homogeneous blend system. This uniformity suggests that the morphological disparities between the blend's two components diminish significantly, making them almost indistinguishable, as noted by Roland and Nagi. Occasionally, this homogeneity can render DSC incapable of distinguishing the T_g of each component within the blend [38]. The blending of EPDM and LLDPE adheres to the "Rule of mixing", manifesting as a shift in the T_g of pure LLDPE towards higher temperatures, a change attributed to the interaction between the two polymer components that restricts molecular chain mobility [39]. An increase in filler content is associated with a notable upward shift in the T_g of the composite materials. In particular T_g of unfilled polymeric blend is -30.2°C where as T_g for composite containing 50 phr of carbon black (filled polymeric blend) is -51.9°C . So it is clearly noticed a significant increment in T_g by 20.24°C with the addition of carbon black. Moreover, the different types of functional groups in VCB aid in dispersing the filler evenly through the interfaces of the blend elements and the distinct phases of EPDM and LLDPE, thus improving the interaction between the filler and the

polymer. The extensive surface area of the carbon black also enhances its specific interactions with the components of the blend.

Thermogravimetric analysis

Thermogravimetric analysis (TGA) is a fundamental technique to determine polymer composites' operational lifespan under elevated temperatures. The thermogravimetric analysis (TGA) and differential thermogravimetric (DTG) graphs for the systems filled with VCB are displayed in Fig. 3a and b, respectively. The decomposition temperature of unfilled and filled EPDM-LLDPE composites are shown in Table 5. The initial breakdown temperature (T_i) of the unfilled blend was observed to be 440°C , whereas the temperature at which it experienced a 50% weight loss (T_{50}) was found to be 492°C . For 5Phr carbon black loading, T_i shows 440°C , whereas for 50 phr loading, T_i becomes 450°C . Thus, 50 phr carbon black loading increases the composite's thermal stability by 10°C . The improvement in thermal stability is attributed to the enhancement of the polymer component by creating three-dimensional network structures. This enhancement is made possible by physical cross-linking with carbon black, resulting in a noticeable increase in heat resistance. This effect likely arises from carbon black nanoparticles' improved dispersion and distribution. Additionally, there is enhanced physical interaction between the filler and the rubber chains. This interaction reduces the mobility of the rubber chains. Carbon black is recognized for its high resistance to heat. Incorporating into

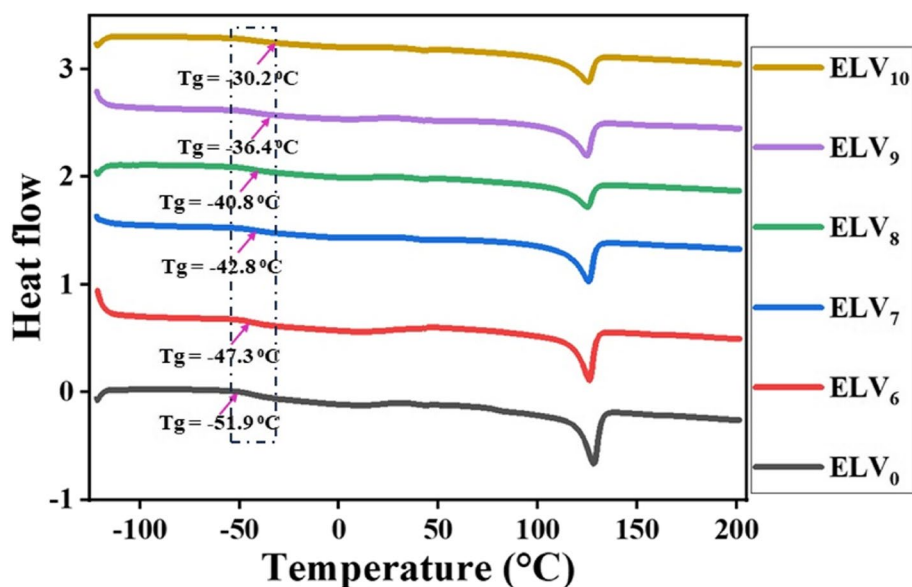


Fig. 2 DSC studies show that adding VCB to composites elevates the glass transition temperature (T_g) relative to the EPDM-LLDPE blend, while an excessively high filler content decreases the melting point of the composite materials

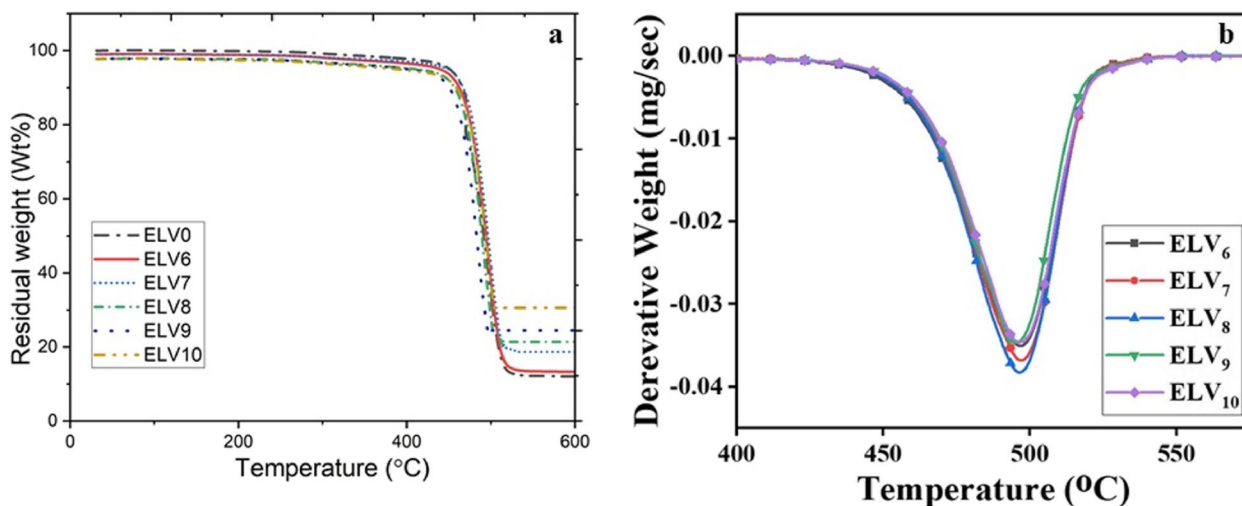


Fig. 3 **a** Thermogravimetric analysis (TGA) curve and **b** differential thermogravimetric (DTG) graph for EPDM-LLDPE composites, both without and with VCB filler

Table 5 Decomposition temperature of VCB-filled EPDM-LLDPE composites

| Sample | T ₅ (°C) | T ₃₀ (°C) | T ₅₀ (°C) | T _{max} (°C) |
|--------|---------------------|----------------------|----------------------|-----------------------|
| ELV0 | 440 | 481.2 | 492.1 | 511.0 |
| ELV6 | 450.7 | 485.7 | 496.8 | 522.2 |
| ELV7 | 468.0 | 487.4 | 497.5 | 529.4 |
| ELV8 | 469.8 | 488.8 | 500.2 | 536.8 |
| ELV9 | 468.6 | 488.6 | 499.2 | 545.1 |
| ELV10 | 469.5 | 489.5 | 502.1 | 545.8 |

Table 6 Surface energy of EPDM, LLDPE, VCB at 180 °C

| Name of the Components | Total surface energy γ (dyne/cm) | Dispersive component γ_d (dyne/cm) | Polar component γ_p (dyne/cm) |
|------------------------|---|---|--------------------------------------|
| EPDM | 38.67 | 36.70 | 1.97 |
| LLDPE | 29.50 | 27.50 | 1.90 |
| VCB | 55.00 | 49.00 | 6.00 |

thermoplastic elastomeric matrix boosts their capacity to tolerate high temperatures. Within composite materials, the distribution of carbon black particles establishes a barrier, protecting the material from heat damage. These particles limit the movement of the polymer molecular chains, which slows down the degradation commonly seen at elevated temperatures.

Calculation of interfacial energy

In blends of immiscible polymers, the placement of fillers can create distinct properties even at minimal filler levels. The method of double percolation significantly improves conductivity and electromagnetic interference (EMI) shielding effectiveness through targeted or interface-specific filler distribution. The determination of filler positioning is crucially influenced by thermodynamic considerations, encapsulated by the Wetting Parameter (ω). According to Young’s equation, the wetting parameter (ω) is a measure of the thermodynamic preference at equilibrium (Eq. 1).

$$\omega_{(A-B)} = \frac{\gamma_{(f-B)} - \gamma_{(f-A)}}{\gamma_{(A-B)}} \tag{1}$$

Where, $\gamma_{(f-B)}$, $\gamma_{(f-A)}$, and $\gamma_{(A-B)}$, are the interfacial tensions between filler-polymer B, filler - polymer A, and polymer A-polymer B interface, respectively. If the wetting parameter ω surpasses 1, it signifies that the filler is predominantly found in polymer A, while a ω value below -1 suggests it’s selectively positioned in polymer B. A specific or pivotal condition arises when ω ’s value falls within the range of -1 to +1, causing the filler to be situated at the interface of the polymer. To ascertain the wetting parameter ω for the VCB-added EPDM/LLDPE blend, an analysis of the surface energy for both polymers and fillers was conducted. This analysis took into account the surface tension of each polymer at a working temperature of 180 °C, as detailed in Table 6. Calculations for the interface-specific terms in the wetting parameter equation utilized both the geometric mean (Eq. 2, Table 7) and the harmonic mean (Eq. 3, Table 7). The geometric mean is typically more relevant for polymer systems filled with substances that exhibit a substantial disparity in surface energy, while the harmonic mean is more suitable for neat polymer blends with minor

Table 7 Interfacial energy between VCB-DPM, VCB-LLDPE, and EPDM-LLDPE at 180 °C

| Component 1 | Component 2 | geometric mean γ_{12} (dyne/cm) | harmonic mean γ_{12} (dyne/cm) |
|-------------|-------------|--|---------------------------------------|
| EPDM | LLDPE | 0.76 | 1.42 |
| EPDM | VCB | 1.98 | 3.81 |
| LLDPE | VCB | 4.33 | 8.28 |

Table 8 Wetting coefficient calculation

| Specification | ω_a^i (geometrical mean) | ω_a^{ii} (harmonic mean) |
|----------------|---------------------------------|---------------------------------|
| EPDM/LLDPE/VCB | 3.092 | 3.14 |

surface energy differences. The derivation of a positive wetting coefficient through both harmonic and geometric means indicates that VCB is predominantly localized within the EPDM portion of the blend, as detailed in Table 8.

$$\gamma_{12} = \gamma_1 + \gamma_2 - 2\sqrt{\gamma_{1d}\gamma_{2d}} - 2\sqrt{\gamma_{1p}\gamma_{2p}} \tag{2}$$

$$\gamma_{12} = \gamma_1 + \gamma_2 - 4\frac{\gamma_{1d}\gamma_{2d}}{\gamma_{1d} + \gamma_{2d}} - 4\frac{\gamma_{1p}\gamma_{2p}}{\gamma_{1p} + \gamma_{2p}} \tag{3}$$

Morphological analysis

Figure 4 illustrates the morphological characteristics of the ELV composite with filler, highlighting how the filler particles are dispersed within the composite blend. At lower filler concentrations, there is an inability for the conductive particles to establish a fully interconnected network inside the EL blend. Despite this minimal interaction between filler and polymer, the filler particles are still evenly distributed across both phases, leading to an increase in elongation at break but a decrease in mechanical strength. On the other hand, a higher concentration of filler enhances its dispersion and achieves a more uniform spread of VCB across the blend, contributing to improved thermal stability and stronger filler-polymer interactions. These benefits translate into increased tensile strength albeit with reduced elongation. The key to determining the filled composites’ electrical properties lies in the effective spread of filler particles. FESEM images from Fig. 4a-d illustrate that a low amount of filler does not succeed in establishing a three-dimensional network of clustered particles (Fig. 4b). However, with a higher quantity of filler, a network connecting the particles becomes evident, which assists in the movement of free electrons across the composite matrix (Fig. 4c). At elevated filler levels (Fig. 4d), reduced clumping is noticeable compared to a conventional polymer blend, likely due to an optimal distribution of filler throughout the blend. The choice of polymer types, filler materials, and dispersion methods is crucial in determining the final characteristics of the composites filled with these materials.

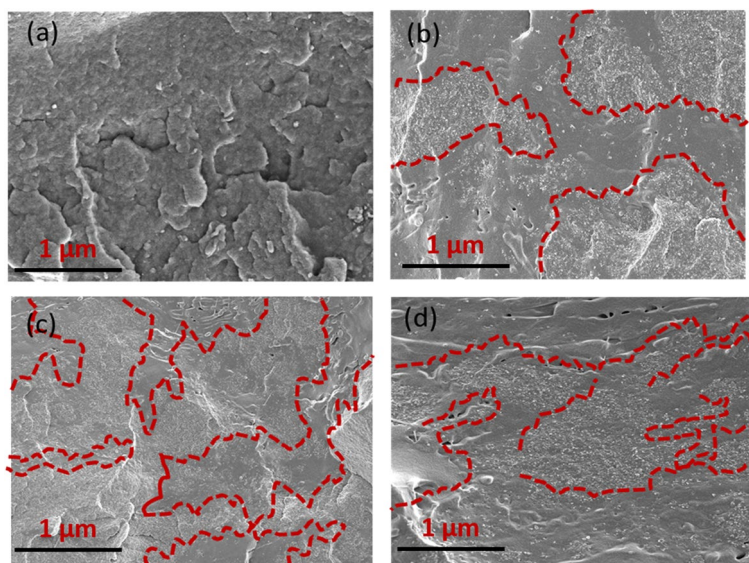


Fig. 4 FESEM micrographs of various quantities of VCB-filled ELV composites at **a** ELV0 **b** ELV 20, **c** ELV 30, **d** ELV 40 respectively

Electrical property

The percolation limit of polymer nanocomposites can be largely determined by measuring DC electrical conductivity. In most cases, pristine polymers and blends work as insulating materials. With the addition of conductive filler, the resistivity of the polymer matrix starts to decrease. The concentration and kind of conductive filler, its dispersion or alignment in the polymer matrix, the characteristics of the polymer, and the processing conditions all impact a polymeric composite material's electrical properties. The formation of a connecting network between the filler particles and the final composite morphology is a critical factor in determining the electrical conductivity. Figure 5a illustrates how the amount of VCB affects the DC conductivity of the ELV blend. A typical percolation graph may be seen while examining the impact of Vulcan XC 72, conducting carbon black on the DC conductivity of an EPDM/LLDPE/VCB composite in Fig. 5b. Pure EPDM/LLDPE blend (ELV₀) exhibits DC conductivity in order of 10⁻¹⁵ S/cm, Initially, the conductivity does not increase substantially with the addition of VCB into the blend i.e. up to 10 phr of VCB content, because the VCBs are not close enough to generate a continuous electron transmission path. Later, A quick increase is observed with further addition due to the continuous compact conductive network that is being

formed. The electrical percolation threshold is the filler concentration at which a filler-filler conductive network forms in the polymer matrix. Once the conductive network forms at the percolation threshold concentration, adding more filler simply increases the number of these networks. However, adding extra filler beyond the percolation threshold only slightly increases the material's conductivity.

$$\sigma^p = \sigma^o (p - p_c)^t \text{ for } p > p_c \tag{4}$$

Power law, Eq. (4), was used to determine the electrical percolation threshold. Here, σ_p gives the DC conductivity, and σ_o is a constant quantity. The p and p_c represent filler fraction and filler fraction at critical or percolation concentration, respectively, and t is the critical exponent. Figure 5b expressed the best-fitted data for the classical power law formula [40]. The percolation threshold of the VCB-filled EPDM/LLDPE 60:40 composites was obtained at 15 phr by applying the classical conduction model. This low percolation threshold manifests the genesis of a three-dimensional interconnected conductive network of VCB nanoparticles within a particular phase of the TPE blend. At the percolation threshold point, the deposited VCB nanoparticles within the rubber phase were uniform enough. The dispersion, along with the

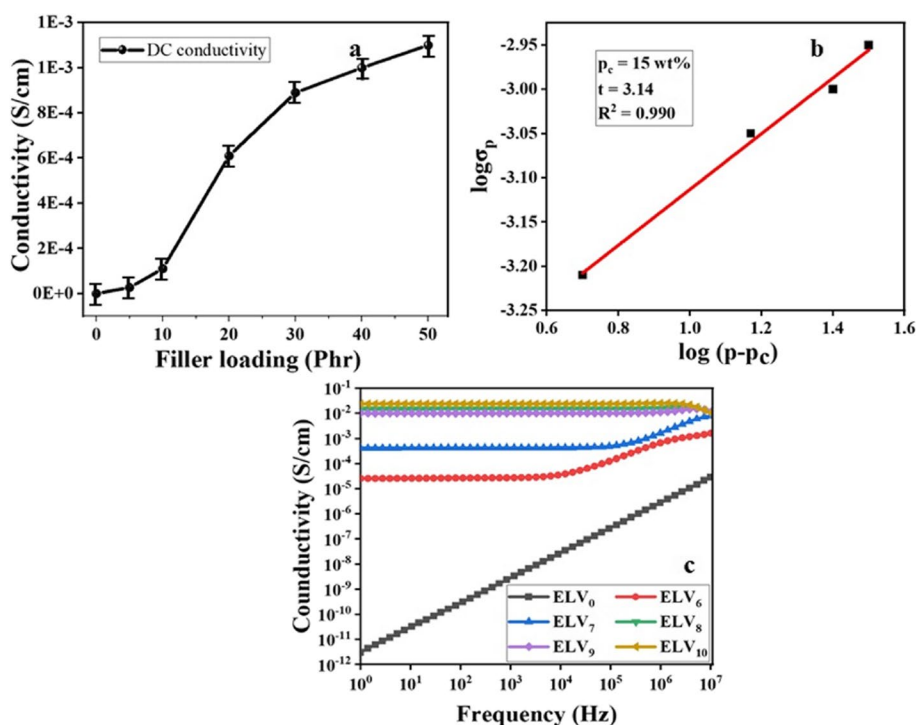


Fig. 5 a DC conductivity of the composite loaded with VCB, b log plot of DC conductivity, c AC conductivity at different filler loading at different frequencies

distribution of VCB in the rubber phase, not only boosts the connectivity of the VCB~VCB and VCB~LLDPE phase for tuning the DC and AC electrical properties but also influences the EMI shielding effectiveness. Figure 5c depicts the correlation between alternating current (AC) conductivity and frequency for the blend and its composites with varying filler loadings. The AC conductivity of the composite material demonstrates a notable enhancement with the augmentation of the filler quantity. The conductivity of the polymer composite with varying percentages of conductive VCB filler exhibits a rise in alternating current (AC) as the frequency decreases.

Conversely, the polymer composite exhibits frequency-independent behavior at higher VCB filler loading. Decreased concentrations of VCB lead to the separation of individual carbon black particles. Nevertheless, when the concentration of electrons is increased, it can result in their excitation and subsequent migration between conducting sites. This phenomenon facilitates the establishment of a more efficient network for electrical conductivity. Once the percolation threshold is exceeded, a network of interconnected VCB particles forms within the polymer matrix. This network facilitates the movement of electrons through conductive spots, resulting in behavior that is not dependent on frequency.

EMI shielding effectiveness (EMI SE)

The Investigation focused on evaluating the ability of polymer nanocomposites to attenuate incoming electromagnetic (EM) waves by studying their EMI shielding effectiveness behavior. The logarithmic relationship between the power of incoming electromagnetic radiation (P_i) and the power of transmitted radiation (P_t) is commonly stated in decibels.

$$SE_T(dB) = -10\log_{10}\frac{P_i}{P_t} = 10\log_{10}\frac{1}{|S_{12}|^2} \quad (5)$$

The quantity of conductive nanofiller and the thickness of the composites are critical factors that contribute significantly to the demonstration of exceptional shielding capabilities and reduced transmission of radiation. In general, electromagnetic radiations impinge upon the leading surface of shielding materials. A portion of the incident electromagnetic radiation is reflected, while another portion is dispersed and absorbed as energy. A specific portion undergoes internal reflection within the material while the remaining quantity is transmitted. When shielded with such material, electromagnetic interference (EMI) shielding effectiveness (SE) refers to its capacity to attenuate radiated electromagnetic waves. The overall shielding efficiency is partitioned into three distinct components, namely absorption (SE_A), reflection (SE_R), and multiple reflections (SE_M). The equations

employed in the determination of the coefficients of absorption (A), reflection (R), and transmission (T) were derived.

$$R = |S_{11}|^2 = |S_{22}|^2 \quad (6)$$

$$T = |S_{21}|^2 = |S_{12}|^2 \quad (7)$$

The summing of SE_A , SE_R , and SE_M denotes the comprehensive measure of shielding effectiveness. Based on the Schelkunoff principle, it is possible to exclude the consideration of multiple reflections (SE_M) in practical electromagnetic interference (EMI) radiation shielding applications under the condition that the shielding efficacy exceeds -10 dB and the thickness of the shielding material surpasses the skin depth of said material. Total electromagnetic interference (EMI) shielding can be measured by utilizing the formulae below.

$$SE_{Total} = SE_A + SE_R \quad (8)$$

$$SE_T(dB) = 10\log_{10}\frac{1}{T} = 10\log_{10}\frac{1}{|S_{21}|^2} = 10\log_{10}\frac{1}{|S_{12}|^2} \quad (9)$$

The pristine blend state has inadequate performance in shielding electromagnetic (EM) radiation, as seen by its shielding efficacy statistics measuring less than -2 dB (Fig. 6a). The variation in electromagnetic interference (EMI) shielding efficiency is linked to changes in the amount of conductive carbon black used. With just a small amount of VCB (10 phr), the composites exhibit an impressive shielding performance of -14.28 dB, allowing the ELV6 to block over 99% of incoming electromagnetic (EM) radiation within the X frequency band. For applications requiring high levels of protection, such as in satellites, medical devices, and radar communication systems, an effective shielding level is typically above -20 dB, which translates to less than one percent of the incoming EM waves being transmitted. Introducing 30 phr of carbon black into the polymer blend results in a shielding effectiveness of -23.71 dB at a thickness of only 1 mm, satisfying the commercial criteria for the use of smart electronics in consumer products. This concentration of filler showcases an excellent capability to absorb 99.9 percent of EM radiation. The enhancement in EM wave attenuation within polymer nanocomposites is governed by key factors. Primarily, the optimal distribution and dispersion of conductive carbon black in the polymer through melt mixing facilitates the formation of a three-dimensional conductive network across the nanocomposite. Moreover, the superior conductivity of VCB plays a vital role in augmenting this attenuation effect. The transport of charges or electrons across

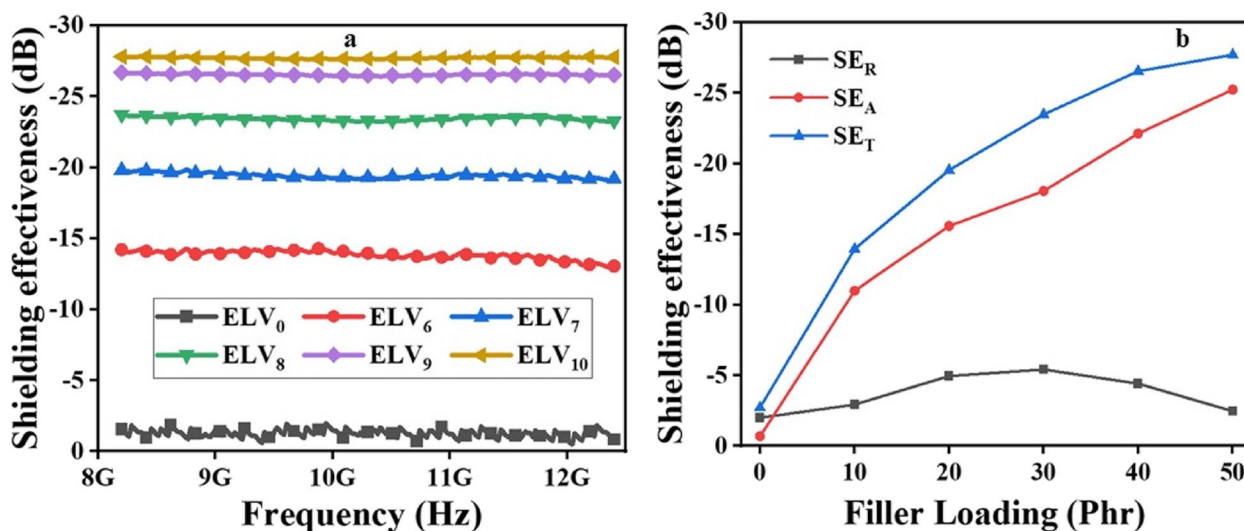


Fig. 6 a Fluctuation in the total EMI shielding efficiency of ELV/VCB, b Influence of filler content on the total shielding effectiveness (SE_T), shielding effectiveness due to absorption (SE_A), and shielding effectiveness due to reflection (SE_R) at a frequency of 10 GHz

the conductive network is boosted with an increased amount of VCB (as depicted in Fig. 6b). In addition, the extensive surface area of the conductive carbon black enhances polarization, the retention of electrical charge, interfacial bonding, and the dissipation of charge within the polymer matrix. A comparison of EMI SE in various polymer blends is provided in the supplementary information (Table S1), illustrating the shielding effectiveness achieved with different formulations.

Conclusions

The study provides an in-depth examination of the TPE blend composed of EPDM and LLDPE. Among various compositions, the 60/40 EPDM/LLDPE blend stands out for displaying superior thermoplastic elastomeric characteristics. We have extensively explored the impact of varying concentrations of carbon black (VCB) in ELV composites to develop a cost-effective, resilient, and flexible material for EMI shielding in industrial uses. The FESEM analysis confirmed the appropriate distribution of VCB within the composite. Our detailed investigation underscores the significant influence of polymer and filler selection, the quantity of filler, and the method of filler distribution on the ultimate characteristics of ELV composites. From the comprehensive evaluation of our experimental findings, it is evident that producing ELV composites through melt blending is an effective approach for manufacturing an affordable, durable, lightweight, and flexible EMI shielding material. Particularly, achieving a shielding effectiveness (SE) of -33.5 dB in samples that are

merely 2 mm thick with a Vulcan Carbon Black (VCB) content of up to 50 phr indicates that this approach is well-suited for widespread use, fulfilling the criteria for commercial feasibility.

Supplementary Information

The online version contains supplementary material available at <https://doi.org/10.1186/s42252-024-00053-7>.

Supplementary Material 1.

Acknowledgements

Narayan Chandra Das thanks the Science and Engineering Research Board (SERB) and the Government of India (CRG/2021/003146) for funding this research work. The authors thank Mr. Soumo Das of Haldia Petrochemicals, India, for providing raw materials.

Authors' contributions

Sreeja Nath Choudhury: Conceptualization, Methodology, Investigation, Data curation, Writing – original draft, Formal analysis, Validation. Jasomati Nayak: Data curation. Palash Das: Writing – review & editing. Aparajita Pal: Writing – review & editing. Ankur Katheria: Resources. Pallab Banerji: Writing – review & editing. Narayan Ch. Das: Conceptualization, Supervision, Writing – review & editing, Funding acquisition.

Availability of data and materials

Datasets can be accessed upon request.

Declarations

Competing interests

The authors declare no competing interests.

Author details

¹Rubber Technology Centre, Indian Institute of Technology, Kharagpur 721302, India. ²Materials Science Centre, Indian Institute of Technology, Kharagpur 721302, India.

Received: 31 October 2023 Accepted: 2 March 2024
Published online: 01 April 2024

References

- M.P. Vidyashree, K. Sushmita, P. Nagarajan, M.K. Kokila, S. Bose, Mimicking 'sea-urchin' like hierarchical carbon structures self-assembled from carbon fibers for green EMI shielding. *Chem. Eng. J. Adv.* **13**, 100430 (2023). <https://doi.org/10.1016/J.CEJA.2022.100430>
- R. Ravindren, S. Mondal, K. Nath, N.C. Das, Investigation of electrical conductivity and electromagnetic interference shielding effectiveness of preferentially distributed conductive filler in highly flexible polymer blends nanocomposites. *Compos. Part A Appl. Sci. Manuf.* **118**, 75–89 (2019). <https://doi.org/10.1016/J.COMPOSITESA.2018.12.012>
- S. Maiti, N.K. Shrivastava, S. Suin, B.B. Khatua, Polystyrene/MWCNT/graphite nanoplate nanocomposites: efficient electromagnetic interference shielding material through graphite nanoplate-MWCNT-graphite nanoplate networking. *ACS Appl. Mater. Interfaces* **5**, 4712–4724 (2013). <https://doi.org/10.1021/am400658h>
- Z. Dou, G. Wu, X. Huang, D. Sun, L. Jiang, Electromagnetic shielding effectiveness of aluminum alloy-fly ash composites. *Compos. Part A Appl. Sci. Manuf.* **38**, 186–191 (2007). <https://doi.org/10.1016/J.COMPOSITESA.2006.01.015>
- P. Bhawal, S. Ganguly, T.K. Das, S. Mondal, S. Choudhury, N.C. Das, Superior electromagnetic interference shielding effectiveness and electro-mechanical properties of EMA-IRGO nanocomposites through the in-situ reduction of GO from melt blended EMA-GO composites. *Compos. B Eng.* **134**, 46–60 (2018). <https://doi.org/10.1016/J.COMPOSITESB.2017.09.046>
- J.T. Orasugh, S.S. Ray, Functional and structural facts of effective electromagnetic interference shielding materials: a review. *ACS Omega* **8**, 8134–8158 (2023). <https://doi.org/10.1021/acsomega.2c05815>
- R. Wilson, G. George, K. Joseph, An introduction to materials for potential EMI shielding applications: status and future, in *Materials for potential EMI shielding applications: processing, properties and current trends*. (2020), pp.1–8. <https://doi.org/10.1016/B978-0-12-817590-3.00001-4>
- P. Das, A. Katheria, J. Nayak, A. Pal, B. Roy, S. Paul, S. Biswas, N.C. Das, Stretchable and lightweight 2D MXene-based elastomeric composite foam for suppressing electromagnetic interference. *J. Alloys Compd.* **976**, 173011 (2024). <https://doi.org/10.1016/J.JALLCOM.2023.173011>
- K. Nath, S.K. Ghosh, P. Das, A. Katheria, N.C. Das, Fabrication of lightweight and biodegradable EMI shield films with selective distribution of 1D carbonaceous nanofiller into the co-continuous binary polymer matrix. *J. Mater. Sci.: Mater. Electron.* **34**, 1–22 (2023). <https://doi.org/10.1007/S10854-023-10212-4>
- R.J. Spontak, N.P. Patel, Thermoplastic elastomers: fundamentals and applications. *Curr. Opin. Colloid Interface Sci.* **5**, 333–340 (2000). [https://doi.org/10.1016/S1359-0294\(00\)00070-4](https://doi.org/10.1016/S1359-0294(00)00070-4)
- S. Amin, M. Amin, Thermoplastic elastomeric (TPE) materials and their use in outdoor electrical insulation. *Rev. Adv. Mater. Sci.* **29**, 15–30 (2011)
- H. Panigrahi, P.R. Sreenath, D.K. Kotnees, Unique compatibilized thermoplastic elastomer with high strength and remarkable ductility: effect of multiple point interactions within a rubber-plastic blend. *ACS Omega* **5**, 12789–12808 (2020). <https://doi.org/10.1021/ACSOMEGA.0C00423>
- S.S. Banerjee, A.K. Bhowmick, Tailored nanostructured thermoplastic elastomers from polypropylene and fluoroelastomer: morphology and functional properties. *Ind. Eng. Chem. Res.* **54**, 8137–8146 (2015). <https://doi.org/10.1021/ACS.IECR.5B01176>
- Y. Wang, Q.M. He, Y.N. Gao, T.N. Yue, M. Wang, Achieving remarkable enhancement on electromagnetic shielding performance in multi-walled carbon nanotube/polydimethylsiloxane composites via adding a small amount of metal micro-particles as scattering points. *Compos. Part A Appl. Sci. Manuf.* **162**, 107135 (2022). <https://doi.org/10.1016/J.COMPOSITESA.2022.107135>
- S. Ganguly, S. Ghosh, P. Das, T.K. Das, S.K. Ghosh, N.C. Das, Poly(N-vinylpyrrolidone)-stabilized colloidal graphene-reinforced poly(ethylene-co-methyl acrylate) to mitigate electromagnetic radiation pollution. *Polym. Bull.* **77**, 2923–2943 (2020). <https://doi.org/10.1007/s00289-019-02892-y>
- S.K. Ghosh, K. Nath, S. Paul, T. Ghosh, N.C. Das, Investigation of the effect of electron beam irradiation on tensile, thermal and gas barrier properties of graphene nanoplatelet loaded thermoplastic nanocomposite films. *Radiat. Phys. Chem.* **214**, 111310 (2024). <https://doi.org/10.1016/J.RADPHYSOCHEM.2023.111310>
- A. Katheria, P. Das, S.K. Ghosh, J. Nayak, K. Nath, S. Paul, S. Biswas, N.C. Das, Fabrication of 2D nanomaterial reinforced co-continuous binary blend composites for thermal management and EMI shielding applications. *J. Polym. Res.* **30**(12), 459 (2023). <https://doi.org/10.1007/S10965-023-03843-Y>
- G.P. Kar, S. Biswas, R. Rohini, S. Bose, Tailoring the dispersion of multiwall carbon nanotubes in co-continuous PVDF/ABS blends to design materials with enhanced electromagnetic interference shielding. *J. Mater. Chem. A Mater.* **3**, 7974–7985 (2015). <https://doi.org/10.1039/C5TA01183C>
- H. Zhang, Z. Heng, J. Zhou, Y. Shi, Y. Chen, H. Zou, M. Liang, In-situ co-continuous conductive network induced by carbon nanotubes in epoxy composites with enhanced electromagnetic interference shielding performance. *Chem. Eng. J.* **398**, 125559 (2020). <https://doi.org/10.1016/J.CEJ.2020.125559>
- P. Das, A. Katheria, J. Nayak, S. Das, K. Nath, S.K. Ghosh, K. Naskar, N.C. Das, Facile preparation of self-healable and recyclable multilayered graphene-based nanocomposites for electromagnetic interference shielding applications. *Colloids Surf. A Physicochem. Eng. Asp.* **676**, 132244 (2023). <https://doi.org/10.1016/j.colsurfa.2023.132244>
- Y. Kou, A.T. Cote, J. Liu, X. Cheng, C.W. Macosko, Robust networks of interfacial localized graphene in cocontinuous polymer blends. *J. Rheol. (N Y N Y)* **65**, 1139–1153 (2021). <https://doi.org/10.1122/8.0000294>
- H. Cheng, Z. Lu, Q. Gao, Y. Zuo, X. Liu, Z. Guo, C. Liu, C. Shen, PVDF-Ni/PE-CNTs composite foams with co-continuous structure for electromagnetic interference shielding and photo-electro-thermal properties. *Eng. Sci.* **16**, 331–340 (2021). <https://doi.org/10.30919/ES8D518>
- A. Katheria, J. Nayak, N.C. Das, A journey of thermoplastic elastomer nanocomposites for electromagnetic shielding applications: from bench to transitional research. *Mater. Adv.* **3**, 2670–2691 (2022). <https://doi.org/10.1039/D1MA00989C>
- Y. Yao, S. Jin, H. Zou, L. Li, X. Ma, G. Lv, F. Gao, X. Lv, Q. Shu, Polymer based lightweight materials for electromagnetic interface shielding: a review. *J. Mater. Sci.* **56**, 6549–6580 (2021). <https://doi.org/10.1007/s10853-020-05635-x>
- K. Nath, S.K. Ghosh, A. Katheria, P. Das, S.N. Chowdhury, P. Hazra, S. Azam, N.C. Das, Design of interconnected 1D nanomaterials with selective localization in biodegradable binary thermoplastic nanocomposite films for effective electromagnetic interference shielding effectiveness. *Polym. Adv. Technol.* **34**, 1019–1034 (2023). <https://doi.org/10.1002/PAT.5949>
- P.C. Ma, M.Y. Liu, H. Zhang, S.Q. Wang, R. Wang, K. Wang, Y.K. Wong, B.Z. Tang, S.H. Hong, K.W. Paik, J.K. Kim, Enhanced electrical conductivity of nanocomposites containing hybrid fillers of carbon nanotubes and carbon black. *ACS Appl. Mater. Interfaces* **1**, 1090–1096 (2009). <https://doi.org/10.1021/AM9000503>
- J.R. Tao, D. Yang, Y. Yang, Q.M. He, B. Fei, M. Wang, Migration mechanism of carbon nanotubes and matching viscosity-dependent morphology in Co-continuous Poly(lactic acid)/Poly(ϵ -caprolactone) blend: Towards electromagnetic shielding enhancement. *Polymer (Guildf)* **252**, 124963 (2022). <https://doi.org/10.1016/j.polymer.2022.124963>
- S.K. Ghosh, T.K. Das, S. Ganguly, S. Paul, K. Nath, A. Katheria, T. Ghosh, S. Nath Chowdhury, N.C. Das, Carbon nanotubes and carbon nanofibers based co-continuous thermoplastic elastomeric blend composites for efficient microwave shielding and thermal management. *Compos. Part A Appl. Sci. Manuf.* **161**, 107118 (2022). <https://doi.org/10.1016/J.COMPOSITESA.2022.107118>
- S.N. Choudhury, P. Das, P. Bhawal, A. Pal, P. Banerji, N.C. Das, Double percolation behavior through the preferential distribution of conductive black in polymer blends to boost electrical properties and EMI shielding effectiveness. *Mater. Today Commun.* **35**, 106109 (2023). <https://doi.org/10.1016/J.MTCOMM.2023.106109>
- A. Karekar, R. Pommer, B. Prem, C. Czibula, C. Teichert, G. Trimmel, K. Saalwächter, NMR-based cross-link densities in EPDM and EPDM/ULDPE blend materials and correlation with mechanical properties. *Macromol. Mater. Eng.* **307**, 2100968 (2022). <https://doi.org/10.1002/MAME.20210968>

31. P. Das, A. Katheria, S. Ghosh, B. Roy, J. Nayak, K. Nath, S. Paul, N.C. Das, Self-healable and super-stretchable conductive elastomeric nanocomposites for efficient thermal management characteristics and electromagnetic interference shielding. *Synth. Met.* **294**, 117304 (2023). <https://doi.org/10.1016/J.SYNTHMET.2023.117304>
32. P. Das, A. Katheria, A. Jana, M. Das, B. Roy, J. Nayak, K. Nath, S.K. Ghosh, A. De, N.C. Das, Super-stretchable, self-healing 2D MXene-based composites for thermal management and electromagnetic shielding applications. *ACS Appl. Eng. Mater.* **1**, 1186–1200 (2023). <https://doi.org/10.1021/ACSAENM.3C00016>
33. A. Katheria, P. Das, J. Nayak, K. Nath, S.K. Ghosh, S. Paul, N.C. Das, Tailored distribution of 1D nanoparticles in co-continuous EMA/TPO flexible polymeric blends used as emerging materials for suppressing electromagnetic radiation. *J. Phys. Chem. Solids* **179**, 111395 (2023). <https://doi.org/10.1016/J.JPCS.2023.111395>
34. A. Katheria, P. Das, S. Paul, K. Nath, S. Kumar Ghosh, N. Ch Das, *Preferential localization of conductive filler in ethylene-co-methyl acrylate/thermoplastic polyolefin polymer blends to reduce percolation threshold and enhanced electromagnetic radiation shielding over K band region* (2022). <https://doi.org/10.1002/pc.27191>
35. T. Saleesung, P. Saeoui, C. Sirisinha, Mechanical and thermal properties of thermoplastic elastomer based on low density polyethylene and ultra-fine fully-vulcanized acrylonitrile butadiene rubber powder (UFNBRP). *Polym. Test.* **29**, 977–983 (2010). <https://doi.org/10.1016/J.POLYMERTESTING.2010.08.008>
36. P. Ghosh, B. Chattopadhyay, A.K. Sen, Thermoplastic elastomers from blends of polyethylene and ethylene-propylene-diene rubber: influence of vulcanization technique on phase morphology and vulcanizate properties. *Polymer (Guildf)* **35**, 3958–3965 (1994). [https://doi.org/10.1016/0032-3861\(94\)90281-X](https://doi.org/10.1016/0032-3861(94)90281-X)
37. H. Ismail, Suryadiansyah, Properties of polypropylene/natural rubber/recycle rubber powder blends. *Polym. Plast. Technol. Eng.* **41**, 833–845 (2002). <https://doi.org/10.1081/PPT-120014391>
38. M. Sumita, K. Sakata, S. Asai, K. Miyasaka, H. Nakagawa, Heterogeneous distribution of conductive particles in polymer blends studied by electron microscopy. *Sen'i Gakkaishi* **47**(8), 384–7 (1991). https://doi.org/10.2115/fiber.47.8_384
39. P. Bhawal, S. Ganguly, T.K. Chaki, N.C. Das, Synthesis, and characterization of graphene oxide filled ethylene methyl acrylate hybrid nanocomposites. *RSC Adv.* **6**(25), 20781–90 (2016). <https://doi.org/10.1039/c5ra24914g>
40. P. Das, A. Katheria, K. Naskar, N.C. Das, Recyclable and super-stretchable conductive elastomeric composites with a carbon nanostructure interconnected network structure for effective thermal management and excellent electromagnetic wave suppressor. *Polym.-Plast. Technol. Mater.* **00**, 1–20 (2023). <https://doi.org/10.1080/25740881.2023.2169160>

Publisher's Note

Springer Nature remains neutral with regard to jurisdictional claims in published maps and institutional affiliations.